Article

Polaritons under Extensive Disordered Gas-Phase Molecular Rotations in a Fabry−Pérot Cavity

Wei Liu, Jingqi Chen, and Wenjie Dou*

Cite This: *J. Phys. Chem. C* 2024, 128, 12544−12550

Read Online

ACCESS | 📊 Metrics & More | 📖 Article Recommendations

ABSTRACT: Directly simulating a large number of molecules interacting with cavity modes is important to understand the polariton chemistry. However, such a task is challenging due to the steep scaling of the computational cost as a function of the number of molecules. Here, we simulate the dynamics and spectra of 1 million gas-phase molecules in a Fabry−Pérot cavity, each weakly interacting with light. We emphasize the effects of molecular rotations and disorder on the polariton dynamics and spectra. Our calculations reveal the existence of the collective effects in the spectra despite the disorder and rotations. Increasing rotational frequencies leads to larger Rabi splitting between lower and upper polaritons, whereas random rotational phases reduce this splitting. These findings await validation in gas-phase polariton experiments.
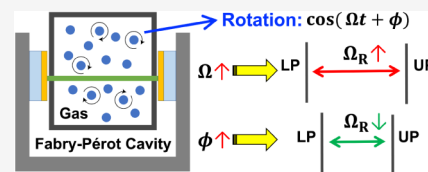
INTRODUCTION

Polaritons, which are hybrid states resulting from the exchange of energy between a light-excited transition in matter and the confined photon mode of an optical cavity,[1−5] exhibit strong light−matter coupling. This coupling is evidenced by distinct peaks observed in the transmission spectrum of the cavity, with these peaks separated by the vacuum Rabi splitting frequency (Ω_R).[6,7] Initially observed in cold atoms[8] and semiconductors,[9] polariton chemistry has recently expanded to include cavity-coupled solution-phase molecules. This exciting development has sparked significant interest and enthusiasm within the scientific community.[1,2,4,5,10−33]

Recent research has revealed that when molecules are coupled to optical cavities, the molecules exhibit distinct energetics, reactivity, and photochemistry compared to their counterparts in free space.[1,3,4,10] Of particular interest is the concept of strong coupling of molecular vibrations, which offers a promising approach for achieving mode-selective chemistry without the need for direct laser excitation. This concept, known as vibrational strong coupling (VSC), was first demonstrated in 2015 by the Ebbesen[34] and Simpkins[35,36] groups using Fabry−Pérot cavities. Since then, a growing body of theoretical and experimental research studies[37−43] has demonstrated reduced reaction rates,[44−46] modified branching ratios,[20] and altered equilibrium constants[47] for thermal, solution-phase reactions under VSC.

While these observations of cavity-altered chemistry are intriguing, there is still intense discussion within the scientific community regarding the underlying mechanisms and reproducibility. Experimental studies on VSC have predominantly focused on condensed-phase systems, where solvent effects, complex mechanisms, and detailed theoretical treatments present challenges.[4,5,48−51] To overcome these challenges, investigating polariton behavior in the gas phase offers

an opportunity to study cleaner and more isolated systems, facilitating a better theoretical understanding of the underlying mechanisms involved.[5,25,52−55]

Recent progress has shown the successful accomplishment of VSC in gas-phase methane (CH_4) by coupling it to a Fabry−Pérot cavity.[56,57] However, the influence of molecular rotations on polaritons remains poorly understood, as there are currently no analytical results available for the linear response of molecular polaritons in the regime of extensively disordered molecules with free rotations.[49,58−60]

In this study, we investigate the behavior of polaritons in a Fabry−Pérot cavity containing one million gas-phase molecules and a single photon. Our focus is on understanding the effects of molecular rotations and level disorder on the dynamic properties and spectral characteristics of polaritons. Through comprehensive theoretical simulations and calculations, we analyze how molecular rotations and disorder impact the frequencies and dephasing time of polaritonic states. This analysis provides valuable insights into the robustness of these states and their potential applications in gas-phase polaritons.
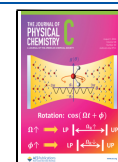
MODEL AND METHOD

Floquet Tavis−Cummings Model. As shown in Figure 1, we investigated the behavior of gas-phase molecules confined within a Fabry−Pérot cavity, taking into account their
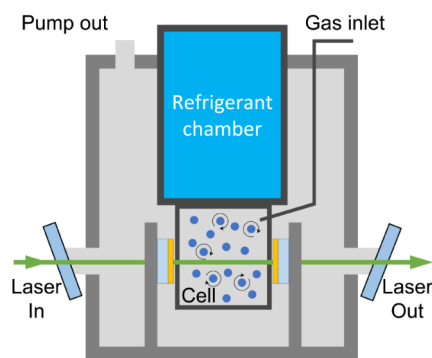
Figure 1. Our theoretical model is based on the setup that employs a cryogenic buffer gas cell apparatus to facilitate cavity coupling of a gas-phase molecular sample.[56,57] This apparatus resides within a vacuum chamber and is enveloped by a Fabry−Pérot optical cavity, enabling strong in situ coupling.

rotational motion.[61,62] The dipole moments of these molecules can be influenced by the molecular geometries, and we can capture the impact of molecular rotations by incorporating a cosine (or sine) function. To model the system, we utilized a single-mode Tavis−Cummings (TC) model with periodic driving, defined by the Hamiltonian $\hat{H} = \hat{H}_M + \hat{H}_C + \hat{H}_{MC}$, where

$$\hat{H}_M = \sum_{j=1}^{N_M} \hbar\omega_j \hat{B}_j^\dagger \hat{B}_j, \qquad \hat{H}_C = \hbar\omega_c \hat{a}^\dagger \hat{a},$$

$$\hat{H}_{MC} = \sum_{j=1}^{N_M} g_c \cos(\Omega t + \phi)\hat{B}_j^\dagger \hat{a} + \text{H. c.}$$

(1)

In the Hamiltonian of molecules $\hat{H}_M$, $\hat{B}_j$ is the annihilation operator for the vibrational mode of the jth molecule. The vibrational energy of the jth molecule $\hbar\omega_j$ are distributed according to a Gaussian function with mean value ω_m, and the level disorder can be represented by standard deviation σ. The level disorder here is the disorder of the vibrational frequencies of the molecules due to inhomogeneous broadening. We define the range of the Gaussian distribution of molecular energies as ΔE. In the Hamiltonian of cavity $\hat{H}_C$, the light field is quantized by the photonic operators $\hat{a}$ (under the single mode approximation). The light−matter interaction in $\hat{H}_{MC}$ is given by $g_c \cos(\Omega t + \phi)$, where Ω means the molecular rotational frequency, and ϕ means the molecular rotational phase. We omit counter-rotating light−matter coupling terms in the Hamiltonian because the collective coupling strength is insufficient for these terms to have a significant impact.[63,64] To simplify the calculation of the Schrödinger equation, we leveraged the temporal periodicity of molecular rotations and applied the Floquet theory,[65−71] which allows us to transform the original time-dependent Hamiltonian $\hat{H}(t)$ into a time-independent Floquet Hamiltonian $\hat{H}^F$:

$$\hat{H}^F = \sum_{n,m=-N_F}^{N_F} (\hat{H}_0 + n\hbar\Omega \otimes \hat{I})\delta_{nm}$$
$$+ \hat{H}_1\left(\frac{1}{2}e^{-i\phi}\delta_{n,m+1} + \frac{1}{2}e^{i\phi}\delta_{n,m-1}\right)$$

(2)

where $\hat{H}_0$ means the diagonal part of $\hat{H}$, and $\hat{H}_1$ means the off-diagonal part of $\hat{H}$ removing $\cos(\Omega t + \phi)$. $\hat{I}$ is the identity matrix. Dirac delta function δ is used. N_F is the number of Floquet levels. By doing so, we can effectively handle the time evolution of the system and the energy levels we calculate correspond to the Floquet quasi-energy levels.[72]

Sparse Matrix Framework. In our study, we specifically focused on molecular rotations and energetic disorder within a system consisting of $N_M \geq 10^6$ molecules and $N_C = 1$ cavity mode. When dealing with such a large-scale system, the primary concern shifts from computational speed to memory usage.[73] To address this, we adopted a memory-efficient approach that takes advantage of the sparsity of the Floquet Hamiltonian $\hat{H}^F$, which has the dimensions of $(2N_F + 1)(N_M + N_C) \times (2N_F + 1)(N_M + N_C)$. Specifically, we utilized the coordinate format (COO) sparse matrix framework,[74] which stores only the nonzero elements (data) and their corresponding coordinates (row and column) in the matrix, denoted as $\hat{H}_s^F$. The total number of nonzero elements in this sparse matrix representation is given by $3 \times (2N_F + 1)(N_M + N_C)$. This approach not only alleviates memory constraints but also enhances computational efficiency by performing matrix multiplications solely on the nonzero elements.

Density of States. For the single-mode TC model, upper polariton (UP) and lower polariton (LP) exist on both sides of the dark states (DS). To handle this, we employed the implicitly restarted Lanczos method[75,76] to calculate half ($k/2$) eigenvalues (represented as Λ) and their corresponding eigenvectors (represented as U) from each end of the spectrum of the sparse matrix H_s^F, instead of diagonalizing the entire matrix. The implicit restart Lanczos method is an iterative algorithm used to solve the eigenvalues and eigenvectors of large symmetric matrices, which improves computational efficiency by regularly restarting.[75,76] This method acts as a wrapper for the ARPACK,[77] SSEUPD, and DSEUPD functions.[78] Then, the density of states (DOS) ρ of polaritons can be written as

$$\rho(\omega) = \text{Tr}[\delta(\tilde{H} - \omega)U^\dagger P_C U]$$

(3)

where $\tilde{H} = \textbf{diag}(\Lambda)$ and **diag** means diagonal matrix mapping. $P_C = |\psi_C^F(0)\rangle\langle\psi_C^F(0)|$ is the projection operator to the cavity (photon) space, and the pth element of $|\psi_C^F(0)\rangle$ is

$$\left|\psi_C^F(0)\right\rangle_p = \begin{cases} 1/\sqrt{N_C} & \text{if } p \in \mathbf{M}, \\ 0 & \text{otherwise} \end{cases}$$

(4)

Here,

$$\mathbf{M} = \{k \in \mathbb{Z} | \text{start}(q) \leq k < \text{end}(q), \ q \in \mathbb{Z}, \ q \in [-N_F, N_F]\}$$

and

$$\text{start}(q) = (N_M + N_C)(q + N_F),$$
$$\text{end}(q) = (N_M + N_C)(q + N_F) + N_C$$

(5)

Before taking the trace, the delta function $\delta(\cdot)$ was initially implemented numerically with Gaussian regularization.[79−81] The Gaussian regularization can be interpreted as applying a Gaussian line-broadening to the traditional time correlation function. The density of states was then directly related to this transformed function by a specific transform:
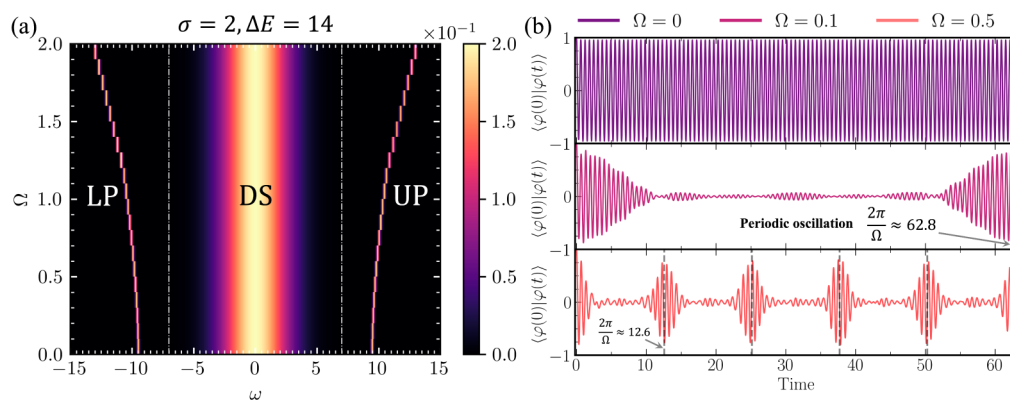
Figure 2. (a) Normalized DOS (heat map) with respect to energy frequency ω under different molecular rotational frequencies Ω. The white dotted line represents the truncation position of the Gaussian distribution. ΔE represents the range of disordered molecular energy levels. Note that the amplitude of polariton and molecular DOS has been adjusted to display on the same graph. (b) Time evolution of correlation functions of photon−matter hybrid wave functions φ under different Ω, as defined in eq 9. After introducing molecular rotations, the oscillation period of the photon−matter hybrid states will depend on the molecular rotation period ($\frac{2\pi}{\Omega}$, red dash lines). Parameters: $\Omega = 0, 0.1, 0.5, \phi = 0, k = 30, \hbar = 1, g_c$ = 0.01, $\omega_c = \omega_m = 0, \sigma = 2, \gamma = 0.1, N_F = 3, \Delta t = 0.001, N_M = 10^6$, and $N_C = 1$. We use the relative unit.

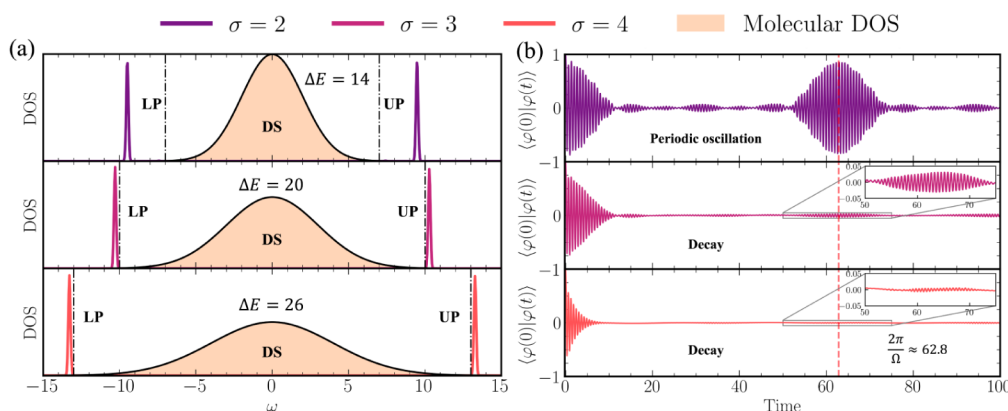**Figure 3.** (a) Normalized DOS with respect to the energy frequency ω under different disorders σ. The black dotted line represents the truncation position of the Gaussian distribution. As the disorder increases, the polarities will become closer to the dark states (DS). ΔE represents the range of disordered molecular energy levels. Note that the amplitude of polariton and molecular DOS has been adjusted to display on the same graph. (b) Time evolution of correlation functions of photon−matter hybrid wave functions φ under different disorders σ, as defined in eq 9. After introducing molecular rotations, the oscillation period of the photon−matter hybrid states will depend on the molecular rotation period ($\frac{2\pi}{\Omega}$, red dash lines). When the disorder increases, the dephasing time of polaritons rapidly decreases and approaches disappearance. Parameters: $\sigma = 2, 3, 4, k = 30, \hbar = 1, g_c = 0.01, \omega_c = \omega_m = 0, \Omega = 0.1, \phi = 0, \gamma = 0.1, N_F = 3, \Delta t = 0.001, N_M = 10^6$, and $N_C = 1$. We use the relative unit.

$$\rho(\omega) = \text{Tr}\left(\int dt \, e^{-i\tilde{H}t} \, e^{i\omega t} \, e^{\gamma^2 t^2/2} U^\dagger P_C U \right)$$

$$= \text{Tr}\left(\frac{1}{\gamma\sqrt{\pi}} e^{-(\tilde{H}-\omega)^2/\gamma^2} U^\dagger P_C U \right) \tag{6}$$

in the small γ (the standard deviation) limit. Through this transformation, we have reduced the originally calculated $(2N_F + 1)(N_M + N_C) \times (2N_F + 1)(N_M + N_C)$ dimensions of DOS to a controllable $k \times k$ dimension of local DOS, greatly reducing computational memory, while not losing the key information we need about polaritons.

Correlation Function. We calculated the correlation function in Hilbert space, but at the same time, we need to use the Floquet Hamiltonian to evolve the wave function in Floquet space, such as

$$i\hbar \frac{\partial |\psi_C^F(t)\rangle}{\partial t} = \hat{H}_s^F |\psi_C^F(t)\rangle \tag{7}$$

So we need a transformation from the wave function in Floquet space to the wave function in Hilbert space:

$$|\varphi(t)\rangle = \frac{1}{2N_F + 1} \sum_{j=-N_F}^{N_F} \exp(i\Omega jt)|\psi_C^F(t)\rangle_{\text{INDEX}(j)} \tag{8}$$

where

$$\text{INDEX}(j) = \{k \in \mathbb{Z} | (j + N_F)(N_M + N_C)$$
$$\leq k < (j + N_F + 1)(N_M + N_C)\}$$

Then, the correlation function of photonic wave function in Hilbert space will be

$$\langle \varphi(0)|\varphi(t)\rangle = \varphi(0)^\dagger \varphi(t) \tag{9}$$

Here, we want to emphasize that without molecular rotations, there exist analytical results of the linear spectra for the TC model.[49,58−60] The numerical method enables us to study the spectra and dynamics of polariton with disorder and
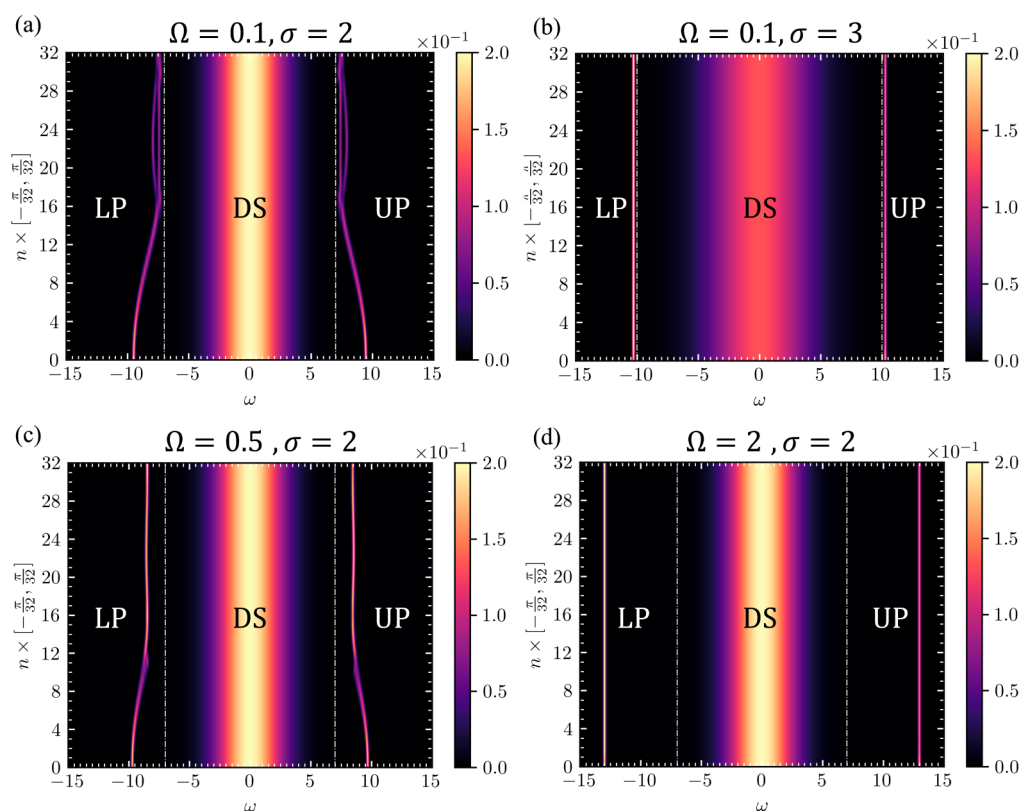
Figure 4. Normalized DOS (heat maps) with respect to the energy frequency ω under different phases ϕ, which are sampled uniformly from $\left[-\frac{n\pi}{32}, \frac{n\pi}{32}\right]$. The larger the number, the greater the disorder of the phase. The white dotted line represents the truncation position of the Gaussian distribution. Parameters: $k = 30$, $\hbar = 1$, $g_c = 0.01$, $\omega_c = \omega_m = 0$, $\gamma = 0.1$, $N_F = 3$, $N_M = 10^6$, and $N_C = 1$. We use the relative unit.

molecular rotations of up to 1 million molecules. Moreover, the numerical method is not limited to the TC model. For a more realistic model that can be used to describe reactivity, no analytical tools are available. The numerical methods presented here can be very helpful to describe the reactivity as well.

■ RESULTS AND DISCUSSION

In Figure 2a, we explore the DOS of polaritons for varying rotational frequencies $\Omega = 0, 0.1, 0.2, \cdots, 2$ with a strong light–matter interaction regime, considering $N_M = 10^6$ molecules coupled to a single cavity mode. In general, we observe that with larger and larger rotational frequencies Ω, the Rabi splitting between LP and UP gets larger and larger. This proves that there is the formation of the rovibrational polariton, which is the effect of the couplings between vibrations, rotations, and light–matter interactions. In Figure 2b, the correlation function of the photonic wave function undergoes substantial changes for $\Omega = 0, 0.1, 0.5$. For $\Omega = 0$, the correlation function evolves uniformly and periodically. As Ω increases, the fluctuation period becomes dominated by a molecular rotational frequency with $T = 2\pi/\Omega$. The change in the fluctuation period from $\Omega = 0.1$ to $\Omega = 0.5$ highlights the profound impact of molecular rotations on polariton state evolution.

In Figure 3a, we investigate the influence of molecular energy disorder (varying σ) on the polariton DOS. As σ increases from 2 to 4, polariton energies deviate significantly from the center of molecular DOS. At the same time, these polaritons are very close to the dark states. The increase in disorder causes the polariton states to mix with the dark

states.[41,82−85] In Figure 3b, we analyze the impact of disorder σ on the correlation function of photons. For $\sigma = 3$ and 4, the correlation function decays close to zero and loses its periodic fluctuations. The fast decay of the polaritonic state that we observed is due to dephasing into the dark states,[86] which depends on the overlap between the polaritons and the dark state manifold.[87]

We want to clarify that there are two kinds of disorder: (1) disorder in the energy of the molecules and (2) disorder in the coupling between the molecules and cavity modes. The first kind of disorder may increase the Rabi splitting as mentioned in the previous study, and the latter will decrease the Rabi splitting.[41,82−85] Here, we find that adding rotations to the coupling between the molecule and cavity modes will increase the Rabi splitting. So, the phenomena we see here are different from the previously reported finding.

In Figure 4a,c, we find that the randomness of the rotational phase tends to shrink the Rabi splitting. Besides, double peaks will appear in the upper and lower polaritons when $\Omega = 0.1$, $\sigma = 2$, and ϕ within the range of $\left(-\frac{\pi}{2}, \frac{\pi}{2}\right)$ to $(-\pi, \pi)$. By increasing Ω to 0.5, the bimodal pattern disappears. Further increasing Ω to 2, UP and LP will significantly move to positions (14 and −14), but UP and LP will no longer approach DS as n increases. As shown in Figure 4b, we increase σ to 3, and its molecular DOS distribution range is within [−10,10], which also produces the phenomenon shown in Figure 4d. But at this point, UP and LP are very close to the edge of DS. From Figure 3b, we know that in this case, UP and LP will quickly decay.

Finally, in Figure 5, under strong disorder, we observe that the introduction of molecular rotations enhances the
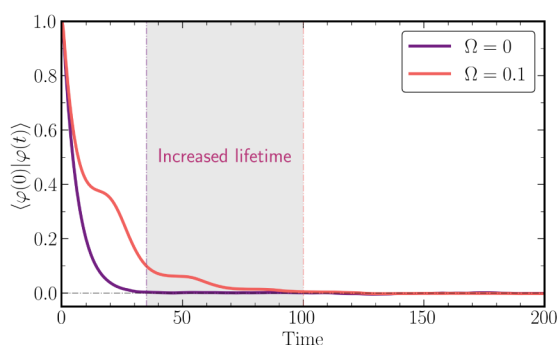

Figure 5. Time evolution of correlation functions of photonic wave functions φ under strong disorder. We observed that molecular rotations increased the dephasing time of the polariton state. Parameters: $\Omega = 0, 0.1$, $k = 30$, $\hbar = 1$, $g_c = 0.0005$, $\omega_c = \omega_m = 0$, $\sigma = 2$, $\gamma = 0.1$, $N_F = 3$, $\Delta t = 0.001$, $N_M = 10^6$, and $N_C = 1$. We use the relative unit.

dephasing time of polariton states. With larger Rabi splitting, the polaritonic states survive against the level disorder of the molecules, such that we observe a longer dephasing time of the polaritonic state in Figure 5.

CONCLUSIONS

In conclusion, our study presents a thorough investigation into the spectra and dynamic behaviors of polaritons influenced by gas-phase molecular rotations and level disorder. Our simulations reveal that even in the presence of disorder and rotations, collective effects manifest in the spectra. Notably, we observed that increasing rotational frequencies leads to larger Rabi splitting between LP and UP, while randomness in rotational phases tends to diminish this splitting. Moreover, the amplification of Rabi splitting proves crucial in bolstering polaritons against molecular-level disorder.

Our findings not only deepen our understanding of polaritonic phenomena but also furnish crucial insights into the advancement and refinement of polaritonic devices. Since we are using the TC model, the chemical reactivity cannot be easily obtained from our results. However, the numerical method presented in the manuscript is general, which does not restrict to the TC model. We hope that we can use the method to study a more realistic model that can be used to describe chemical reactivity.

Additionally, there is considerable interest in exploring the formation of rovibrational polaritons amidst disorder at rotational frequencies. This avenue of research holds promise for uncovering new dimensions of polaritonic behavior and warrants further exploration in forthcoming studies. Last but not least, cavity leakage can be incorporated into our numerical method. One way of incorporating cavity leakage is to model multiple cavity modes instead of just one mode.

ASSOCIATED CONTENT

Data Availability Statement

The code used in the simulation is available on GitHub (https://github.com/Weitheskmt/WeiGPS).

AUTHOR INFORMATION

Corresponding Author

Wenjie Dou − *Department of Chemistry, School of Science and Department of Physics, School of Science, Westlake University, Hangzhou, Zhejiang 310024, China; Institute of Natural Sciences, Westlake Institute for Advanced Study, Hangzhou, Zhejiang 310024, China;* ⓘ orcid.org/0000-0001-5410-6183; Email: douwenjie@westlake.edu.cn

Authors

Wei Liu − *Department of Chemistry, School of Science, Westlake University, Hangzhou, Zhejiang 310024, China; Institute of Natural Sciences, Westlake Institute for Advanced Study, Hangzhou, Zhejiang 310024, China;* ⓘ orcid.org/0009-0006-7686-929X

Jingqi Chen − *Department of Chemistry, School of Science, Westlake University, Hangzhou, Zhejiang 310024, China; Institute of Natural Sciences, Westlake Institute for Advanced Study, Hangzhou, Zhejiang 310024, China*

Complete contact information is available at:
https://pubs.acs.org/10.1021/acs.jpcc.4c02592

Notes

The authors declare no competing financial interest.

REFERENCES

(1) Ebbesen, T. W. Hybrid light−matter states in a molecular and material science perspective. *Acc. Chem. Res.* **2016**, 49, 2403−2412.

(2) Simpkins, B. S.; Dunkelberger, A. D.; Vurgaftman, I. Control, modulation, and analytical descriptions of vibrational strong coupling. *Chem. Rev.* **2023**, 123, 5020−5048.

(3) Garcia-Vidal, F. J.; Ciuti, C.; Ebbesen, T. W. Manipulating matter by strong coupling to vacuum fields. *Science* **2021**, 373, No. eabd0336.

(4) Ribeiro, R. F.; Martínez-Martínez, L. A.; Du, M.; Campos-Gonzalez-Angulo, J.; Yuen-Zhou, J. Polariton chemistry: controlling molecular dynamics with optical cavities. *Chem. Sci.* **2018**, 9, 6325−6339.

(5) Herrera, F.; Owrutsky, J. Molecular polaritons for controlling chemistry with quantum optics. *J. Chem. Phys.* **2020**, 152, 100902.

(6) Dovzhenko, D.; Ryabchuk, S.; Rakovich, Y. P.; Nabiev, I. Light−matter interaction in the strong coupling regime: configurations, conditions, and applications. *Nanoscale* **2018**, 10, 3589−3605.

(7) Hertzog, M.; Wang, M.; Mony, J.; Börjesson, K. Strong light−matter interactions: a new direction within chemistry. *Chem. Soc. Rev.* **2019**, 48, 937−961.

(8) Haroche, S.; Kleppner, D. Cavity quantum electrodynamics. *Phys. Today* **1989**, 42, 24−30.

(9) Skolnick, M.; Fisher, T.; Whittaker, D. Strong coupling phenomena in quantum microcavity structures. *Semicond. Sci. Technol.* **1998**, 13, 645.

(10) Hutchison, J. A.; Schwartz, T.; Genet, C.; Devaux, E.; Ebbesen, T. W. Modifying chemical landscapes by coupling to vacuum fields. *Angew. Chem., Int. Ed.* **2012**, 51, 1592−1596.

(11) Kowalewski, M.; Bennett, K.; Mukamel, S. Non-adiabatic dynamics of molecules in optical cavities. *J. Chem. Phys.* **2016**, 144 (5), 054309.

(12) Galego, J.; Garcia-Vidal, F. J.; Feist, J. Suppressing photochemical reactions with quantized light fields. *Nat. Commun.* **2016**, *7*, 13841.

(13) Kowalewski, M.; Bennett, K.; Mukamel, S. Cavity femtochemistry: Manipulating nonadiabatic dynamics at avoided crossings. *J. Phys. Chem. Lett.* **2016**, *7*, 2050−2054.

(14) Herrera, F.; Spano, F. C. Cavity-controlled chemistry in molecular ensembles. *Phys. Rev. Lett.* **2016**, *116*, 238301.

(15) Feist, J.; Galego, J.; Garcia-Vidal, F. J. Polaritonic chemistry with organic molecules. *ACS Photonics* **2018**, *5*, 205−216.

(16) Du, M.; Martínez-Martínez, L. A.; Ribeiro, R. F.; Hu, Z.; Menon, V. M.; Yuen-Zhou, J. Theory for polariton-assisted remote energy transfer. *Chem. Sci.* **2018**, *9*, 6659−6669.

(17) Campos-Gonzalez-Angulo, J. A.; Ribeiro, R. F.; Yuen-Zhou, J. Resonant catalysis of thermally activated chemical reactions with vibrational polaritons. *Nat. Commun.* **2019**, *10*, 4685.

(18) Lacombe, L.; Hoffmann, N. M.; Maitra, N. T. Exact potential energy surface for molecules in cavities. *Phys. Rev. Lett.* **2019**, *123*, 083201.

(19) Mandal, A.; Huo, P. Investigating new reactivities enabled by polariton photochemistry. *J. Phys. Chem. Lett.* **2019**, *10*, 5519−5529.

(20) Thomas, A.; Lethuillier-Karl, L.; Nagarajan, K.; Vergauwe, R. M.; George, J.; Chervy, T.; Shalabney, A.; Devaux, E.; Genet, C.; Moran, J.; Ebbesen, T. W. others Tilting a ground-state reactivity landscape by vibrational strong coupling. *Science* **2019**, *363*, 615−619.

(21) Wang, D. S.; Yelin, S. F. A roadmap toward the theory of vibrational polariton chemistry. *ACS Photonics* **2021**, *8*, 2818−2826.

(22) Nagarajan, K.; Thomas, A.; Ebbesen, T. W. Chemistry under vibrational strong coupling. *J. Am. Chem. Soc.* **2021**, *143*, 16877−16889.

(23) Simpkins, B. S.; Dunkelberger, A. D.; Owrutsky, J. C. Mode-specific chemistry through vibrational strong coupling (or a wish come true). *J. Phys. Chem. C* **2021**, *125*, 19081−19087.

(24) Chen, T.-T.; Du, M.; Yang, Z.; Yuen-Zhou, J.; Xiong, W. Cavity-enabled enhancement of ultrafast intramolecular vibrational redistribution over pseudorotation. *Science* **2022**, *378*, 790−794.

(25) Dunkelberger, A. D.; Simpkins, B. S.; Vurgaftman, I.; Owrutsky, J. C. Vibration-cavity polariton chemistry and dynamics. *Annu. Rev. Phys. Chem.* **2022**, *73*, 429−451.

(26) Li, T. E.; Cui, B.; Subotnik, J. E.; Nitzan, A. Molecular polaritonics: Chemical dynamics under strong light−matter coupling. *Annu. Rev. Phys. Chem.* **2022**, *73*, 43−71.

(27) Mandal, A.; Krauss, T. D.; Huo, P. Polariton-mediated electron transfer via cavity quantum electrodynamics. *J. Phys. Chem. B* **2020**, *124*, 6321−6340.

(28) Li, X.; Mandal, A.; Huo, P. Theory of mode-selective chemistry through polaritonic vibrational strong coupling. *J. Phys. Chem. Lett.* **2021**, *12*, 6974−6982.

(29) Li, X.; Mandal, A.; Huo, P. Cavity frequency-dependent theory for vibrational polariton chemistry. *Nat. Commun.* **2021**, *12*, 1315.

(30) Pannir-Sivajothi, S.; Campos-Gonzalez-Angulo, J. A.; Martínez-Martínez, L. A.; Sinha, S.; Yuen-Zhou, J. Driving chemical reactions with polariton condensates. *Nat. Commun.* **2022**, *13*, 1645.

(31) Mandal, A.; Li, X.; Huo, P. Theory of vibrational polariton chemistry in the collective coupling regime. *J. Chem. Phys.* **2022**, *156*, 014101.

(32) George, J.; Singh, J. Polaritonic chemistry: Band-selective control of chemical reactions by vibrational strong coupling. *ACS Catal.* **2023**, *13*, 2631−2636.

(33) Ahn, W.; Triana, J. F.; Recabal, F.; Herrera, F.; Simpkins, B. S. Modification of ground-state chemical reactivity via light−matter coherence in infrared cavities. *Science* **2023**, *380*, 1165−1168.

(34) Shalabney, A.; George, J.; Hutchison, J. A.; Pupillo, G.; Genet, C.; Ebbesen, T. W. Coherent coupling of molecular resonators with a microcavity mode. *Nat. Commun.* **2015**, *6*, 5981.

(35) Long, J. P.; Simpkins, B. Coherent coupling between a molecular vibration and Fabry−Perot optical cavity to give hybridized states in the strong coupling limit. *ACS Photonics* **2015**, *2*, 130−136.

(36) Simpkins, B.; Fears, K. P.; Dressick, W. J.; Spann, B. T.; Dunkelberger, A. D.; Owrutsky, J. C. Spanning strong to weak normal mode coupling between vibrational and Fabry−Pérot cavity modes through tuning of vibrational absorption strength. *ACS Photonics* **2015**, *2*, 1460−1467.

(37) Xiang, B.; Ribeiro, R. F.; Dunkelberger, A. D.; Wang, J.; Li, Y.; Simpkins, B. S.; Owrutsky, J. C.; Yuen-Zhou, J.; Xiong, W. Two-dimensional infrared spectroscopy of vibrational polaritons. *Proc. Natl. Acad. Sci. U. S. A.* **2018**, *115*, 4845−4850.

(38) Xiang, B.; Ribeiro, R. F.; Li, Y.; Dunkelberger, A. D.; Simpkins, B. B.; Yuen-Zhou, J.; Xiong, W. Manipulating optical nonlinearities of molecular polaritons by delocalization. *Sci. Adv.* **2019**, *5*, No. eaax5196.

(39) Xiang, B.; Ribeiro, R. F.; Chen, L.; Wang, J.; Du, M.; Yuen-Zhou, J.; Xiong, W. State-selective polariton to dark state relaxation dynamics. *J. Phys. Chem. A* **2019**, *123*, 5918−5927.

(40) Hu, W.; Gustin, I.; Krauss, T. D.; Franco, I. Tuning and enhancing quantum coherence time scales in molecules via light-matter hybridization. *J. Phys. Chem. Lett.* **2022**, *13*, 11503−11511.

(41) Pérez-Sánchez, J. B.; Mellini, F.; Yuen-Zhou, J.; Giebink, N. C. Collective polaritonic effects on chemical dynamics suppressed by disorder. *Phys. Rev. Res.* **2024**, *6*, 013222.

(42) Engelhardt, G.; Cao, J. Unusual dynamical properties of disordered polaritons in microcavities. *Phys. Rev. B* **2022**, *105*, 064205.

(43) Sukharev, M.; Subotnik, J.; Nitzan, A. Dissociation slowdown by collective optical response under strong coupling conditions. *J. Chem. Phys.* **2023**, *158*, 084104.

(44) Thomas, A.; George, J.; Shalabney, A.; Dryzhakov, M.; Varma, S. J.; Moran, J.; Chervy, T.; Zhong, X.; Devaux, E.; Genet, C.; Hutchison, J. A. others Ground-state chemical reactivity under vibrational coupling to the vacuum electromagnetic field. *Angew. Chem* **2016**, *128*, 11634−11638.

(45) Hirai, K.; Takeda, R.; Hutchison, J. A.; Uji-I, H. Modulation of Prins cyclization by vibrational strong coupling. *Angew. Chem.* **2020**, *132*, 5370−5373.

(46) Ahn, W.; Herrera, F.; Simpkins, B. *Modification of urethane addition reaction via vibrational strong coupling*, ChemRxiv; 2022.

(47) Pang, Y.; Thomas, A.; Nagarajan, K.; Vergauwe, R. M.; Joseph, K.; Patrahau, B.; Wang, K.; Genet, C.; Ebbesen, T. W. On the role of symmetry in vibrational strong coupling: the case of charge-transfer complexation. *Angew. Chem., Int. Ed.* **2020**, *59*, 10436−10440.

(48) Climent, C.; Feist, J. On the sn 2 reactions modified in vibrational strong coupling experiments: Reaction mechanisms and vibrational mode assignments. *Phys. Chem. Chem. Phys.* **2020**, *22*, 23545−23552.

(49) Mandal, A.; Taylor, M. A.; Weight, B. M.; Koessler, E. R.; Li, X.; Huo, P. Theoretical advances in polariton chemistry and molecular cavity quantum electrodynamics. *Chem. Rev.* **2023**, *123*, 9786−9879.

(50) Schäfer, C.; Flick, J.; Ronca, E.; Narang, P.; Rubio, A. Shining light on the microscopic resonant mechanism responsible for cavity-mediated chemical reactivity. *Nat. Commun.* **2022**, *13*, 7817.

(51) Campos-Gonzalez-Angulo, J. A.; Poh, Y. R.; Du, M.; Yuen-Zhou, J. Swinging between shine and shadow: Theoretical advances on thermally activated vibropolaritonic chemistry. *J. Chem. Phys.* **2023**, *158*, 230901.

(52) Szidarovszky, T.; Badankó, P.; Halász, G. J.; Vibók, A. ́. Nonadiabatic phenomena in molecular vibrational polaritons. *J. Chem. Phys.* **2021**, *154*, 064305.

(53) Fischer, E. W.; Saalfrank, P. Cavity-induced non-adiabatic dynamics and spectroscopy of molecular rovibrational polaritons studied by multi-mode quantum models. *J. Chem. Phys.* **2022**, *157*, 034305.

(54) Gu, Y.; Gu, B.; Sun, S.; Yong, H.; Chernyak, V. Y.; Mukamel, S. Manipulating attosecond charge migration in molecules by optical cavities. *J. Am. Chem. Soc.* **2023**, *145*, 14856−14864.

(55) Yu, Q.; Bowman, J. M. Manipulating hydrogen bond dissociation rates and mechanisms in water dimer through vibrational strong coupling. *Nat. Commun.* **2023**, *14*, 3527.

(56) Wright, A. D.; Nelson, J. C.; Weichman, M. L. A versatile platform for gas-phase molecular polaritonics. *J. Chem. Phys.* **2023**, *159*, 164202.

(57) Wright, A. D.; Nelson, J. C.; Weichman, M. L. Rovibrational polaritons in gas-phase methane. *J. Am. Chem. Soc.* **2023**, *145*, 5982−5987.

(58) Ćwik, J. A.; Kirton, P.; De Liberato, S.; Keeling, J. Excitonic spectral features in strongly coupled organic polaritons. *Phys. Rev. A* **2016**, *93*, 033840.

(59) Zeb, M. A.; Kirton, P. G.; Keeling, J. Exact states and spectra of vibrationally dressed polaritons. *ACS Photonics* **2018**, *5*, 249−257.

(60) Yuen-Zhou, J.; Koner, A. Linear response of molecular polaritons. *J. Chem. Phys.* **2024**, *160*, 154107.

(61) Spaun, B.; Changala, P. B.; Patterson, D.; Bjork, B. J.; Heckl, O. H.; Doyle, J. M.; Ye, J. Continuous probing of cold complex molecules with infrared frequency comb spectroscopy. *Nature* **2016**, *533*, 517−520.

(62) Changala, P. B.; Weichman, M. L.; Lee, K. F.; Fermann, M. E.; Ye, J. Rovibrational quantum state resolution of the C60 fullerene. *Science* **2019**, *363*, 49−54.

(63) De Liberato, S. Light-matter decoupling in the deep strong coupling regime: The breakdown of the Purcell effect. *Phys. Rev. Lett.* **2014**, *112*, 016401.

(64) Frisk Kockum, A.; Miranowicz, A.; De Liberato, S.; Savasta, S.; Nori, F. Ultrastrong coupling between light and matter. *Nat. Rev. Phys.* **2019**, *1*, 19−40.

(65) Barone, S.; Narcowich, M.; Narcowich, F. Floquet theory and applications. *Phys. Rev. A* **1977**, *15*, 1109.

(66) Mosallanejad, V.; Chen, J.; Dou, W. Floquet-driven frictional effects. *Phys. Rev. B* **2023**, *107*, 184314.

(67) Liu, W.; Chen, Z.-H.; Su, Y.; Wang, Y.; Dou, W. Predicting rate kernels via dynamic mode decomposition. *J. Chem. Phys.* **2023**, *159*, 144110.

(68) Chen, J.; Liu, W.; Dou, W. Floquet Nonadiabatic Nuclear Dynamics with Photoinduced Lorenz-Like Force in Quantum Transport. *J. Phys. Chem. C* **2023**, *128*, 11219−11228.

(69) Wang, Y.; Mosallanejad, V.; Liu, W.; Dou, W. Nonadiabatic dynamics near metal surfaces with periodic drivings: A generalized surface hopping in floquet representation. *J. Chem. Theory Comput.* **2024**, *20*, 644−650.

(70) Bätge, J.; Wang, Y.; Levy, A.; Dou, W.; Thoss, M. Periodically driven open quantum systems with vibronic interaction: Resonance effects and vibrationally mediated decoupling. *Phys. Rev. B* **2023**, *108*, 195412.

(71) Liu, W.; Chen, J.; Dou, W. Enhancement of Chiral-Induced Spin Selectivity via Circularly Polarized Light. *arXiv* **2024**, *2402*, 00903.

(72) Zhou, Z.; Wu, Y.; Bian, X.; Subotnik, J. E. Nonadiabatic Dynamics in a Continuous Circularly Polarized Laser Field with Floquet Phase-Space Surface Hopping. *J. Chem. Theory Comput.* **2023**, *19*, 718−732.

(73) Hager, G.; Wellein, G. *Introduction to high performance computing for scientists and engineers*; CRC Press, 2010.

(74) Langr, D.; Tvrdik, P. Evaluation criteria for sparse matrix storage formats. *IEEE Trans. Parallel Distrib. Sys.* **2016**, *27*, 428−440.

(75) Wu, K.; Simon, H. Thick-restart Lanczos method for large symmetric eigenvalue problems. *SIAM J. Matrix Anal. Appl.* **2000**, *22*, 602−616.

(76) Calvetti, D.; Reichel, L.; Sorensen, D. C. An implicitly restarted Lanczos method for large symmetric eigenvalue problems. *Electron. Trans. Numer. Anal.* **1994**, *2*, 21.

(77) Lehoucq, R. B.; Sorensen, D. C.; Yang, C. *ARPACK Software*. https://github.com/opencollab/arpack-ng.

(78) Lehoucq, R. B.; Sorensen, D. C.; Yang, C. *ARPACK users' guide: Solution of large-scale eigenvalue problems with implicitly restarted Arnoldi methods*; SIAM, 1998.

(79) Weiße, A.; Wellein, G.; Alvermann, A.; Fehske, H. The kernel polynomial method. *Rev. Mod. Phys.* **2006**, *78*, 275.

(80) Bradbury, N. C.; Chuang, C.; Deshmukh, A. P.; Rabani, E.; Baer, R.; Caram, J. R.; Neuhauser, D. Stochastically Realized Observables for Excitonic Molecular Aggregates. *J. Phys. Chem. A* **2020**, *124*, 10111−10120.

(81) Bradbury, N.; Ribeiro, R.; Caram, J. R.; Neuhauser, D. Realistic Polaritons in Large Scale Simulations of Molecular Aggregates. *arXiv* **2023**, *2308*, 04385.

(82) Cohn, B.; Sufrin, S.; Basu, A.; Chuntonov, L. Vibrational polaritons in disordered molecular ensembles. *J. Phys. Chem. Lett.* **2022**, *13*, 8369−8375.

(83) Chen, H.-T.; Zhou, Z.; Sukharev, M.; Subotnik, J. E.; Nitzan, A. Interplay between disorder and collective coherent response: Superradiance and spectral motional narrowing in the time domain. *Phys. Rev. A* **2022**, *106*, 053703.

(84) Schwennicke, K.; Giebink, N. C.; Yuen-Zhou, J. Extracting accurate light−matter couplings from disordered polaritons. *Nanophotonics* **2024**, *13*, 2469−2478.

(85) Sommer, C.; Reitz, M.; Mineo, F.; Genes, C. Molecular polaritonics in dense mesoscopic disordered ensembles. *Phys. Rev. Res.* **2021**, *3*, 033141.

(86) Davidsson, E.; Kowalewski, M. The role of dephasing for dark state coupling in a molecular Tavis−Cummings model. *J. Chem. Phys.* **2023**, *159*, 044306.

(87) Groenhof, G.; Climent, C.; Feist, J.; Morozov, D.; Toppari, J. J. Tracking polariton relaxation with multiscale molecular dynamics simulations. *J. Phys. Chem. Lett.* **2019**, *10*, 5476−5483.